BL12B2
NSRRC BM

BL12B2 is one of the two contract beamlines operated by National Synchrotron Radiation Research Center (NSRRC, Taiwan) under collaborative research with Japan Synchrotron Radiation Research Institute (JASRI) and RIKEN. Although this beamline was originally designed for materials science and protein crystallography, because of the completion of the 3-GeV Taiwan Photon Source (TPS) at NSRRC, the beamtime distribution between these research fields has changed. For the last several years, most of the beamtime has been assigned to material science users, about 75% of whom are from Taiwan. The rest of the beamtime is shared between international users from Japan and around the world. Owing to the COVID-19 pandemic, overseas research travel has been restricted. Most of the beamtime has been canceled and shifted to mail-in operation.

Figure 1 schematically depicts the beamline layout. The beamline is equipped with a collimating mirror (CM), a double crystal monochromator (DCM), and a focusing mirror (FM). The measured spot size and total flux of the beam are about 250 μm^2 and 1.5×10^{11} photons at the protein end-station at an incident photon energy of 12 keV, respectively. Five end-stations, EXAFS, projection X-ray microscopy (PXM), X-ray diffraction, X-ray scattering, and powder X-ray diffraction (powder XRD), are equipped tandemly inside the experimental hutch of BL12B2.

EXAFS experiments are performed at the EXAFS table. The EXAFS spectrum can be measured using both transmission and reflection modes. X-ray scattering experiments can be performed using the HUBER six-circle diffractometer. The sample temperature of X-ray

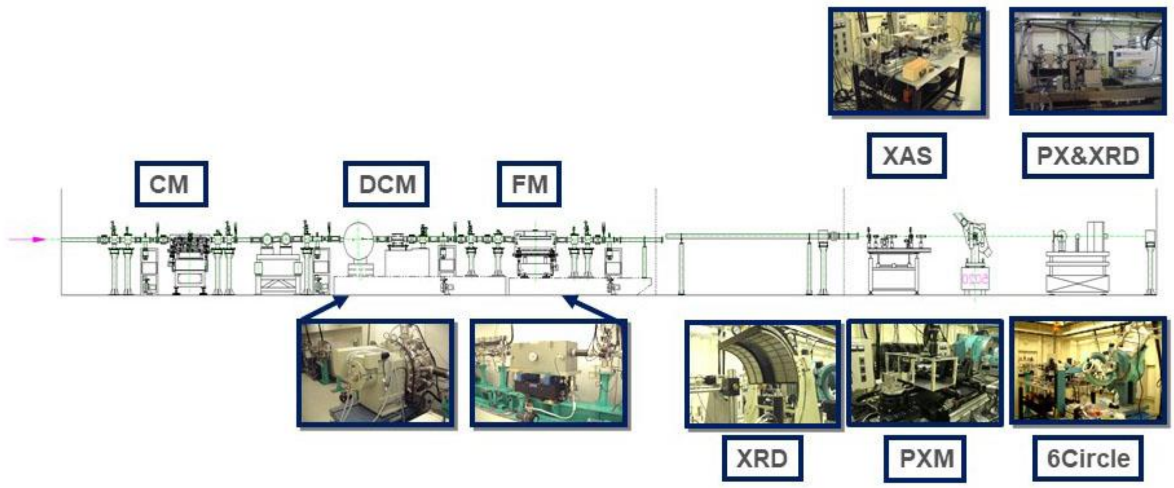

Fig. 1. Schematic layout of BL12B2.

scattering experiment can be changed from 20 to 400 K by using closed cycle cryostat. In 2018, the PXM end-station was installed at the XRD table. High-pressure X-ray diffraction is performed using a CCD camera at the protein crystallography table.

The powder XRD end-station, which is equipped with a CCD and a SPring-8 standard auto–sample-changer system, was installed in FY2009 and used for protein diffraction experiments until FY2017. However, beamtime for protein-crystallography users has diminished since FY2017. Currently, the powder XRD end-station is mainly used by material scientists. The user interface software for powder XRD experiments is the SPring-8 standard BSS software. The CCD detector was upgraded to Raynox MX225-HE in FY2014. Nitrogen gas flow cryostat and heat gun can change the sample temperature from 60 to 500 K. Moreover, a closed cycle He cryostat can be used for low-temperature experiments. Electrodes (AUTOLAB PGSTAT204 (Metrohm)) were prepared for in situ electrochemical experiments. High-pressure experiments can be performed using a plate-type diamond anvil cell (DAC).

Materials science experiments cover a wide range of topics, such as new materials research, energy science, nanoscience, and geophysical science. In FY2021, BL12B2 users published 27 papers in SCI journals [1–27].

BL12B2 is used for in situ or in operando X-ray experiments for research on electrocatalysis [1–3], such as fuel cell [4], battery [5–9], oxygen evolution reaction [10,11], and CO_2 conversion [12] research. Photocatalytic conversion of photsensitive system is reocognized as one of the important technique to solve energy and environment problems. Prof. Hua-Shu Hsu (National Pintung University) and colleagues employed Co sputtering to achieve Co-rich doping on a photosensitive ZnO nanowire surface in order to manipulate its density of state which is key to its catalytic properties [3] (Fig. 2).

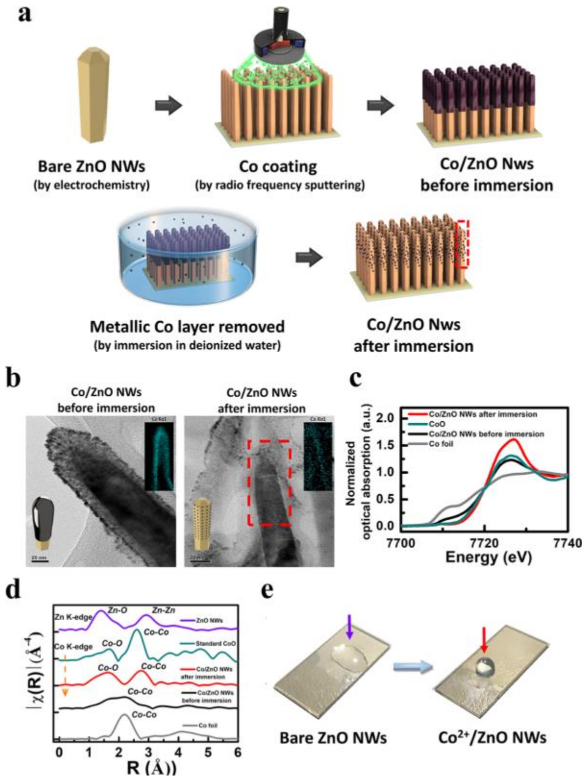

Fig. 2 (a) Synthetic strategy for fabricating Co-rich ZnO nanowire. (b) High-resolution transmission electron microscopy (HRTEM) and mapping energy-dispersive X-ray spectroscopy (EDX) images. (c) Co K-edge XANES spectrum. (d) Radial distribution function (RDF) of Co and Zn sites. (e) Images of hydrophilic–hydrophobic transitions on a ZnO nanowire surface [8].

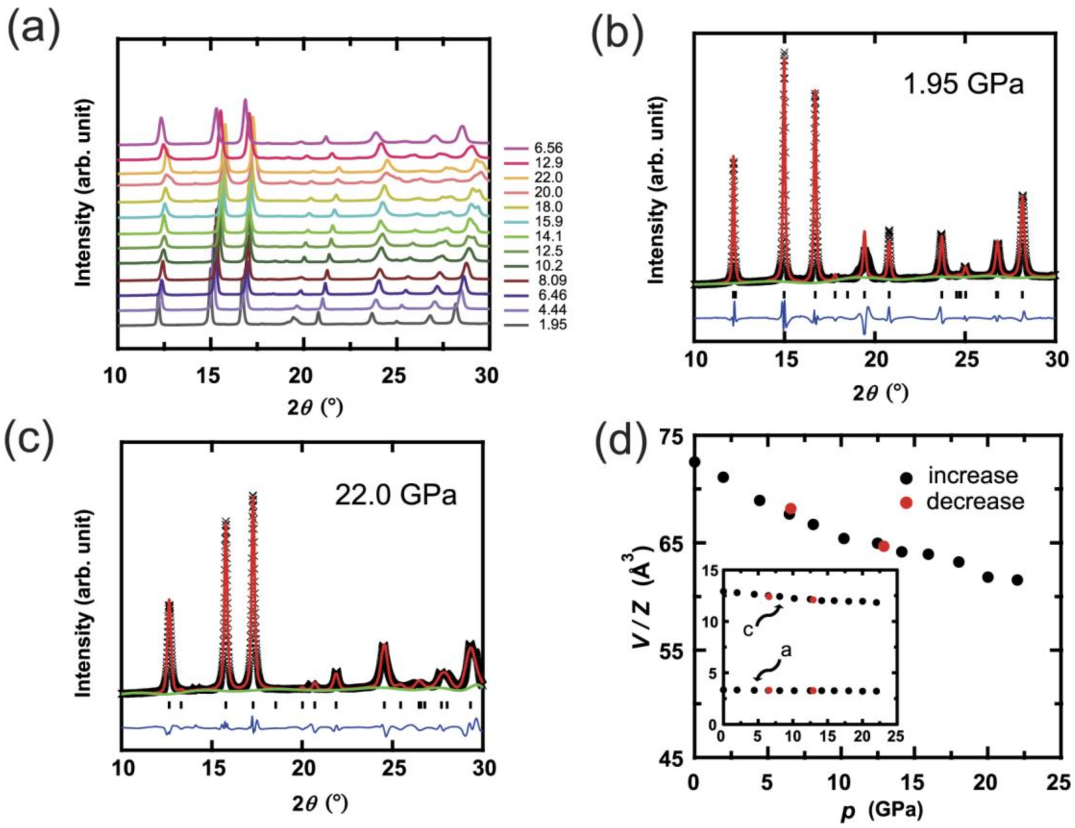

Fig. 3 Pressure-dependent powder XRD patterns of β-PdBi2. (a) Pressure dependence, (b) low pressure phase, (c) high pressure phase, and (d) pressure dependence of a- and c-axes [17].

Other studies have been focused on samples under extreme conditions to investigate a new physical phenomenon [15–22]. New types of topological insulator which exhibits superconductivity are hot topics in the field of solid-state physics. Prof. Kubozono Yoshihiro (Okayama University) and colleagues have studied several topological insulators under pressure. Figure 3 shows the pressure-dependent XRD spectra of the topological insulator β-PdBi2, which exhibits superconductivity at 4.1 K [17]. The same group also studied high-pressure XRD on other samples that exhibit superconducting properties [15–19]. Dr. Yamaoka Hitoshi (RIKEN) and Prof. Mizuki Junichiro (Kwansei Gakuin University) and their colleagues have studied the high-pressure phase of iron-based superconductors [21,22]. User support is provided by two local beamline scientists and one engineer.

Liao Yen-Fa, Yoshimura Masato, Tatsumi Tatsuya, Ishii Hirofumi*
NSRRC, Taiwan

References:

[1] Peng, T., et al. (2021). *J. Am. Chem. Soc*. **143**, 17226.

[2] Lin, Y. J., et al. (2021). *Appl. Phys. Lett.* **119**,

192102.

[3] Lin, J. X., et al. (2021). *ACS Appl. Mater. Interfaces* **13**, 23173.

[4] Kuo, H. C., et al. (2021). *J. Anal. Appl. Pyrol.* **153**, 104991

[5] Guo, R. H., et al. (2021). *Chem. Eng. J.* **414**, 128842.

[6] Abdollahifar, M., et al. (2021). *ACS Sustainable Chem. Eng*. **9**, 13717.

[7] Yeh, N. H., et al. (2021). *ACS Appl. Mater. Interfaces* **13**, 7355.

[8] Hsu, W. D., et al. (2021). *Sci. Rep*. **11**, 1929.

[9] Xie, D., et al. (2021). *Small* **17**, 2007239.

[10] Chala, S. A., et al. (2021). *ACS Nano* **15**, 14996.

[11] Bai, L., et al. (2021). *Nat. Energy* **6**, 1054.

[12] Zhu, C., et al. (2021). *Chem* **7**, 406.

[13] Tsukahara, T., et al. (2021). *J. Appl. Phys*. **130**, 243904.

[14] Sereika, R., et al. (2021). *Dalton Trans*. **50**, 3005.

[15] Taguchi, T., et al. (2021). *Inorg. Chem*. **60**, 3585.

[16] Li, H., et al. (2021). *J. Phys. Chem*. *C* **125**, 20617.

[17] Suzuki, A., et al. (2021). *J. Phys.: Condens. Mater.* **33**, 135702.

[18] Taguchi, T., et al. (2021). *J. Phys: Condens. Mater.* **33**, 485704.

[19] Wang, Y., et al. (2021). *Phys. Chem. Chem. Phys*. **23**, 23014.

[20] Yamaoka, H., et al. (2021). *J. Phys. Soc. Jpn.* **90**, 124801.

[21] Yamamoto, Y., et al. (2021). *J. Phys.: Condens. Mater.* **33**, 255603.

[22] Yamamoto, Y., et al. (2021). *J. Phys.: Condens. Mater*. **33,** 255602.

[23] Li, H., et al. (2021). *Sci. Total Environ*. **783**, 147037.

[24] Choi, S. H., et al. (2021). *J. Am. Chem. Soc.* **143,** 20291.

[25] Guan, H. H., et al. (2021). *Biochem. Biophys. Res. Commun.* **551**, 33.

[26] Guan, H. H., et al. (2021). *Bioinorg. Chem. Appl.* **2021**, 2572844.

[27] Chan, S. I., et al. (2021). *J. Am. Chem. Soc.* **143**, 3359.